Random-phase calculation of the circularly dichroic 3000 Å band of (+)-D-camphor

ARTICLE *in* THE JOURNAL OF CHEMICAL PHYSICS · AUGUST 1978

Impact Factor: 2.95 · DOI: 10.1063/1.436745

Random-phase calculation of the circularly dichroic 3000 Å band of (+)-*D*-camphor[a)]

J. Texter and E. S. Stevens[b)]

Department of Chemistry, State University of New York at Binghamton, Binghamton, New York 13901
(Received 27 March 1978)

Time-dependent Hartree theory is applied in the random-phase, coupled-oscillator approximation to the calculation of the circular dichroism of the carbonyl $\pi^* \leftarrow n$ transition in (+)−*D*-camphor. X-ray evidence indicating a very slight pyramidal distortion of the C(CO)C array in the ground state and the observation of the $00 \leftarrow 000$ member of a $00\nu_s \leftarrow 000$ progression ($\nu'_s \sim 1100$ cm^{-1}) in both absorption ($f \sim 3\times10^{-5}$) and circular dichroism lead us to conclude that a principal component of the $\pi^* \leftarrow n$ transition mechanism is one which is electric-dipole allowed. Each such electric-dipole allowed member is in addition both magnetic-dipole and electric-quadrupole allowed. In coupling the $00\nu_s \leftarrow 000$ $\pi^* \leftarrow n$ transitions to the CC and CH densities of states via a polarizability approximation, it is verified that the circular dichroism arising from the coupling of the electric-dipole transition moment is negligible in comparison with that resulting from the coupling of the magnetic-dipole transition moment with the backbone density of states. Moreover it is shown that the associated electric-quadrupole transition moment dominates the coupling energetics. The observed inhomogeneous dissymmetry, $\Delta\epsilon/\epsilon$, occurs as a result of additional thermally populated $00\nu_s \leftarrow 0\nu_a \cdot 0$ ($\nu''_{a'} \sim 400$ cm^{-1}) and $00\nu_s \leftarrow \nu_{a'} \cdot 00$ ($\nu'_{a'} \sim 500$ cm^{-1}) progressions which contribute appreciably to the absorption intensity but not to the circular dichroism.

I. INTRODUCTION

The absorption (ϵ) and circular dichroism ($\Delta\epsilon$) of ketones in the nonvacuum ultraviolet region have been widely studied theoretically[1-15] and experimentally.[16-18] It is generally accepted that the 3000 Å carbonyl absorption corresponds to a $\pi^* \leftarrow n$ excitation[19] which is strongly magnetic-dipole allowed and on the basis of a C_{2v} analysis of the chromophore often treated as strictly electric-dipole forbidden between zero-point vibronic states. The evolution of quadrant, octant, and antioctant rules itself suggests that symmetry arguments alone cannot reliably explain experimental circular dichroism spectra. Schellman[1] has stressed the need to establish the relative importance of the (static) one-electron,[2-4] the Kuhn–Kirkwood electric-dipole, electric-dipole ($\mu_e\mu_e$),[5-8] and the electric-dipole, magnetic-dipole ($\mu_e\mu_m$) mechanisms of optical rotation in deciding the origins of rotatory power in any particular system. Concerning definition and usage of terms Moscowitz[4] has pointed out that all theoretical formulations leading to or from the Rosenfeld expression for rotatory strength,

$$R_{ij} = -i\langle i|\hat{\mu}_e|j\rangle \cdot \langle j|\hat{\mu}_m|i\rangle, \tag{1.1}$$

are "one-electron" since $\hat{\mu}_e$ and $\hat{\mu}_m$ are one-electron operators. In the classical application of one-electron mechanisms,[2,9] charge distributions emanating from the incomplete screening of perturbing group nuclei are used to mix excited states on otherwise symmetric chromophores in producing optical activity. Höhn and Weigang[10] refer to such mechanisms as static-coupling mechanisms in contrast with dynamical-coupling mechanisms, the latter including both $\mu_e\mu_e$ and $\mu_e\mu_m$ coupled-oscillator formulations.

The origins of optical activity in the 3000 Å band of ketones cannot yet be considered as definitively established since Moscowitz and Snyder,[20,21] by applying the static-coupling mechanism, and Höhn and Weigang,[10] by applying a dynamical-coupling mechanism, have had identical success in rationalizing experimental rotatory strengths for a wide range of carbonyl containing compounds.

Our present interest in the 3000 Å band of (+)−D-camphor was motivated in part by Gillard and Mitchell's report[22] of the vapor phase absorption and circular dichroism spectra, their assignment of the observed vibronic structure to a $00\nu_s \leftarrow 000$ progression in the π^* carbonyl stretching vibration, and questions pertaining to the inhomogeneous dissymmetry

$$g(\nu) = \Delta\epsilon(\nu)/\epsilon(\nu), \tag{1.2}$$

which decreases with increasing frequency over the vibronic envelope. The experimental data are reproduced in Figs. 1 and 2, where the 1100 cm^{-1} progression is evident in both ϵ and $\Delta\epsilon$. Those workers describe the observed absorption intensity as deriving from a mixing of the carbonyl $\pi^* \leftarrow \pi$ and $\pi^* \leftarrow n$ transitions, resulting in a vibronic electric-dipole moment oriented parallel to the carbonyl bond. The inhomogeneity of the dissymmetry ($dg/d\nu \sim -2\times10^{-5}$ cm^{-1}) is accounted for with an electric-dipole forbidden, magnetic-dipole allowed transition mechanism.[22]

In their early study of (+)-D-camphor in hexane, published before the elaboration of Herzberg–Teller intensity borrowing mechanisms, Kuhn and Gore[23] explained the inhomogeneous dissymmetry as arising from the presence in absorption of an adjacent overlapping band having a different origin. Their explanation has occasionally been noted but discounted.[11,22] We present here our appraisal of the relative importance of the varietal mechanisms of optical rotation and vibronic absorption in accounting for the data of Figs. 1 and 2 and the associated transition mechanisms. In the following sections

[a)]This work was supported in part by the National Science Foundation under Grant Nos. PCM-77-19930, 21220 and in part by the U. S. Public Health Service under Grant No. GM-24862-01.

[b)]Previous publications under the name E. S. Pysh.

 0021-9606/78/6904-1680$01.00

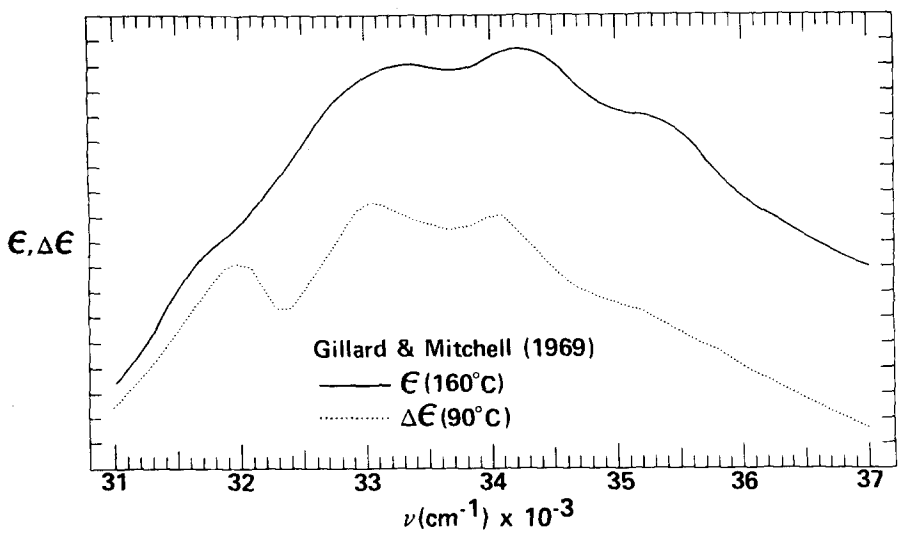

FIG. 1. Vapor phase spectra of (+)–*D*-camphor reported by Gillard and Mitchell (Ref. 22). The data illustrated here were obtained by a careful photographic enlargement of the above authors' original figure, followed by the conversion of abscissa from nm to cm^{-1} at 100 cm^{-1} intervals, followed by the replotting illustrated here. The ordinate scales originally were reported in positive optical density units, and hence are presented here in arbitrary units. The calibrated extinction of room temperature solution spectra reported by Gillard and Mitchell have $\epsilon_{max} \sim 25$ and $\Delta\epsilon_{max} \sim 1.5$.

we present the requisite elements of the time-dependent Hartree method for the calculation of optical properties, the fundamental structural data for (+)-D-camphor, and those transition mechanisms which must be considered as possibly contributing to the observed absorption and circular dichroism.

II. TIME DEPENDENT HARTREE THEORY

The time-dependent Hartree (TDH) theory, as elaborated by McLachlan, Gregor, and Ball[24,25] and Harris,[26] is a generalized susceptibility theory describing the linear response to an applied classical radiation field of a collection of bound electrons (coupled oscillators), and the ensuing equations for ϵ and $\Delta\epsilon$ embed the random-phase approximation. Since, as Harris has pointed out,[26] the property of circular dichroism arises as a result of temporal correlations between the electric-dipole and magnetic-dipole transition moments of the molecule in the absence of applied fields, the TDH theory used here is suitably termed a dynamical-coupling approach in the terminology of Höhn and Weigang.[10]

The TDH theory has been principally used as a vehicle for studying the optical properties of polymers,[27–31] although no such restriction is inherent in the formulation. Instead of considering monomers (of a polymer), in the present application we adopt the independent-systems approach as utilized by Snyder and Johnson in their studies of the vacuum ultraviolet spectra of optically active alcohols,[32] where we consider in zeroth order that the carbonyl group is electronically separable from the rest of the molecule. The insufficiency of first-order treatments of optical rotatory power in molecular systems not satisfying a group separability criterion has been demonstrated by Applequist.[33] Calculations of optical properties arising from interactions between electronically degenerate or nearly degenerate transition densities require that the interaction Hamiltonian be diagonalized exactly or that an equivalently exact computational procedure be used. The 3000 Å absorption bands of saturated, aliphatic ketones exhibit oscillator strengths which vary roughly in the range of 10^{-4}–10^{-3} on passing from formaldehyde to the higher homologs.

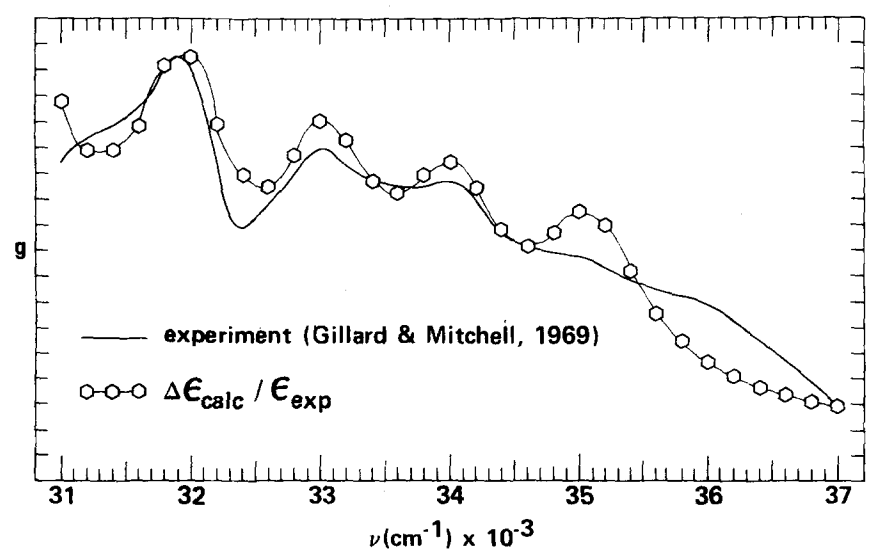

FIG. 2. Vapor phase dissymmetry, $g(\nu) = \Delta\epsilon(\nu)/\epsilon(\nu)$, for (+)–*D*-camphor presented in arbitrary numerical units. The experimental curve was obtained from the data of Fig. 1. The $\Delta\epsilon_{calc}/\epsilon_{exp}$ curve is discussed in Sect. V. It appears that vestiges of a $4 \leftarrow 0$ member exist at approximately 36 100 cm^{-1}.

Hence our separability assumption in the present case is probably a good approximation, and we are by choice neglecting static (one-electron) contributions resulting from delocalization of the carbonyl states over the molecular backbone. The carbonyl group (i.e., those electrons participating in the σ^*, π, π^*, and n orbitals) is presumed to be electronically neutral, and electron exchange between the carbonyl group and the rest of the molecule is ignored. This particular assumption, regarding the carbonyl states, is not a requisite of TDH theory, and a reformulation over a different set of separable delocalized subsystems would be straightforward if required. In the sequel we explicitly consider the "nonbonding" n and π^* antibonding orbitals of the carbonyl group, as well as the implicit contributions to those states from the π and σ^* states induced vibronically. With regard to the rest of the molecule, we consider the remaining CC and CH bonds as forming the second "group." The electronic properties of each of these bonds are represented in the polarizability approximation by a set of orthogonal electric-dipole transition moments having band centers above the aliphatic $\sigma^* \leftarrow \sigma$ (CC) absorption threshold ($\sim 68\,000$ cm^{-1}).[34] Justification already exists for localized orbital treatments of CH and CC bonds,[35,36] and we scale the associated electric-dipole transition moments in conformity with the zero-frequency anisotropic bond polarizabilities[36] as described more fully in Sec. V. Justification for invoking this polarizability approximation to the CC and CH densities of states comes from the separation of the 3000 Å region from the $\sigma^* \leftarrow \sigma$ backbone absorption threshold, and hence it is only the associated 3000 Å dispersion which enters our calculations.

The resulting TDH equations for absorption and circular dichroism,[26] correct to first order in the Coulombic interaction $V_{n_i m_j}$ between transitions $n_i \leftarrow 0_i$ and $m_j \leftarrow 0_j$ on groups i and j, respectively, are

$$\epsilon(\nu)=\frac{8\pi\nu}{3c\hbar}\left\{\sum_{i=1,2}\sum_{n_i}\frac{\langle 0_{n_i}|\hat{\mu}_e|n_i\rangle\cdot\langle n_i|\hat{\mu}_e|0_{n_i}\rangle\nu}{\nu_{n_i}^2-z^2}+4\sum_{n_1}\sum_{m_2}V_{n_1m_2n_1}\frac{\langle n_1|\hat{\mu}_e|0_{n_1}\rangle\cdot\langle 0_{m_2}|\hat{\mu}_e|m_2\rangle\nu_{n_1}\nu_{m_2}}{(\nu_{n_1}^2-z^2)(\nu_{m_2}^2-z^2)}\right\}'', \tag{2.1}$$

$$\Delta\epsilon(\nu)=\frac{-64\pi\nu}{9c\hbar}\left\{\sum_{n_1}\sum_{m_2}\nu_{m_2}V_{n_1m_2}\frac{\mathrm{Im}[\langle 0_{m_2}|\hat{\mu}_e|m_2\rangle\cdot\langle n_1|\hat{\mu}_m|0_{n_1}\rangle]}{(\nu_{n_1}^2-z^2)(\nu_{m_2}^2-z^2)}\right.$$
$$\left.-\frac{1}{2c}\sum_{n_1}\sum_{m_2}\nu_{n_1}\nu_{m_2}zV_{n_1m_2}(\mathbf{R}_{m_2}-\mathbf{R}_{n_1})\cdot\frac{[\langle 0_{m_2}|\hat{\mu}_e|m_2\rangle\times\langle n_1|\hat{\mu}_e|0_{n_1}\rangle]}{(\nu_{n_1}^2-z^2)(\nu_{m_2}^2-z^2)}\right\}''. \tag{2.2}$$

In the above equations π, c, and $\hbar$ are fundamental constants, the frequencies ν, ν_j, and z and the interaction $V_{n_1m_2}$ are expressed in cm^{-1}, the complex frequency $z=\nu+i\delta_j$, where $2\delta_j$ is the half-width of the associated transition ν_j for the transition $j \leftarrow 0_j$, $\hat{\mu}_e$, and $\hat{\mu}_m$ are, respectively, the electric- and magnetic-dipole operators, and Im[...] and $\{...\}''$ denote taking the imaginary part. The $|0_j\rangle$ and $|j\rangle$ refer to the electronic or vibronic ground (initial) and excited states, respectively, for each of the groups ($i=1,2$), where n_1 indexes the vibronic excited states of the carbonyl and m_2 indexes the three orthogonal electric-dipole transition moments centered on the midpoints of each of the CC and CH bonds. The Cartesian vectors $\mathbf{R}_j$ are from an arbitrary molecular fixed origin to the corresponding jth transition center, which in the carbonyl case is fixed on the oxygen nucleus. Since electron exchange and orbital overlap between the bonds are neglected, $V_{n_1m_2}$ represents a Coulombic interaction between the electric-multipolar transition charge density fields of the $n_1 \leftarrow 0_{n_1}$ and $m_2 \leftarrow 0_{m_2}$ transitions. These interactions may be computed when the applied radiation field is zero, and hence in a gauge having a divergence free vector-potential. We chose to evaluate the $V_{n_1m_2}$ classically in the monopole approximation between m_2 associated electric-dipole transition moments and the n_1 associated electric-dipole and electric-quadrupole transition moments as is described more fully in Sec. V. Equations (2.1) and (2.2) derive from the strong coupling limit of Harris' formulation,[26] and their use is justified partly by virtue of some of the $V_{n_1m_j}$ computed being on the order of 1000 cm^{-1}. The cross-sectional units of cm^2/molecule resulting in Eqs. (2.1) and (2.2) were converted to l mol^{-1} cm^{-1} in our calculations (cf. Sec. V). The second term of Eq. (2.2) represents the (electric-dipole, electric-dipole) $\mu_e\mu_e$-coupling optical rotatory mechanism and the first term represents the $\mu_e\mu_m$-coupling mechanism, in close analogy with the older coupled oscillator formalism.[37] We believe that the present study represents the first explicit use of $\mu_e\mu_m$-coupling in the TDH framework.

III. ABSOLUTE CONFIGURATION

The absolute configuration of (+)-D-camphor, illustrated in Fig. 3, has been established by x-ray diffraction[38,39] and x-ray fluorescence[40] of, respectively, (+)-3-bromocamphor and (+)-3-bromocamphor-9(π)-sulfonate monohydrate. The refinement of Allen and Rogers[39] resolved coordinates for the hydrogens attached to the bicyclic backbone. In addition we placed the methyl hydrogens in tetrahedral coordination with CH bond lengths of 1.05 Å, and the $H_{3\text{-}2}$ hydrogen, replacing the substituent bromine, was placed to mirror approximately the coordinates of $H_{6\text{-}2}$. The resulting coordinates for all atoms are listed in Table I, where the methyl groups are set in staggered positions.

The atomic coordinates are used in the evaluation of Eqs. (2.1) and (2.2) as they serve to orient the associated bond transition moments and centers as discussed

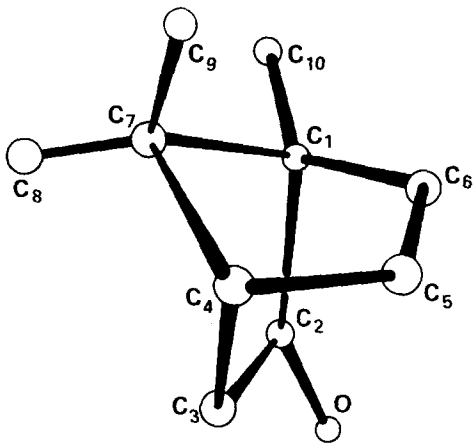

FIG. 3. Atom numbering scheme for (+)–*D*-camphor. Adapted from Allen and Rogers' paper (Ref. 39).

more fully in Sec. V. In addition, however, a result of Allen and Rogers' refinement is that the principal axis of the carbonyl thermal ellipsoid lies out of the $C_1C_2C_3$ plane. Substituted norbornane structures are generally puckered or twisted, and hence we expect that the $C_1(C_2O)C_3$ array is slightly nonplanar in (+)-D-camphor as well. The resulting $C_1C_2C_3$, C_1C_2O, and C_3C_2O valency angles reported are 105.6°, 127.7°, and 126.6°, respectively. This indicates that the oxygen is approximately 4.6° above or below the $C_1C_2C_3$ plane. The coordinates of Table I reflect the intermediate planar configuration; the quantitative effects of the out of plane distortions are discussed in Secs. IV and V. A corollary to those discussions is that there is a finite admixture of *s* character in the C_2 AO contribution to the carbonyl π^* orbital.

TABLE I. Atomic coordinates for (+)–*D*-camphor with the methyl groups in staggered positions.[a]

Atom	*x* (Å)	*y* (Å)	*z* (Å)	Quadrant[b]
O	−1.83	1.35	−1.63	0
C_1	0.	1.12	0.	2
C_2	−1.16	0.67	−0.90	1
C_3	−1.20	−0.87	−0.79	3
C_4	0.	−1.14	0.	3
C_5	1.31	−0.74	−0.77	2
C_6	1.21	0.82	−0.81	2
C_7	0.	0.	1.04	1
C_8	−1.27	0.01	1.91	1
C_9	1.26	0.03	1.93	1
C_{10}	−0.15	2.57	0.44	1
H_3-1[c]	−2.11	−1.22	−0.49	4
H_3-2	−1.40	−1.22	−1.92	3
H_4-1	−0.14	−1.91	0.62	4
H_5-1	2.07	−1.26	−0.17	2
H_5-2	1.26	−0.88	−1.55	3
H_6-1	2.13	1.16	−0.62	2
H_6-2	1.39	1.63	−1.68	2
H_8-1	−1.28	−0.84	2.52	4
H_8-2	−1.28	0.87	2.50	1
H_8-3	−2.12	0.	1.29	4
H_9-1	1.26	−0.81	2.52	1
H_9-2	1.27	0.90	2.56	1
H_9-3	2.12	0.02	1.33	2
H_{10}-1	−1.09	2.71	0.87	1
H_{10}-2	0.60	2.80	1.55	1
H_{10}-3	−0.03	3.20	−0.39	2

[a]The molecular origin is fixed on the nonbonded C_4C_1 line segment with the positive *y* axis directed in the C_4 to C_1 direction. The positive *z* axis passes through bridge carbon C_7.

[b]These quadrant designations are for *xy* quadrants of the oxygen centered carbonyl frame of Fig. 4 as discussed in Secs. IV and V.

[c]The first numeral in the hydrogen designation specifies the bonded carbon.

IV. $\pi^* \leftarrow n$ TRANSITION MECHANISMS

There does not appear to be any serious disagreement over the assignment of the 3000 Å band as a $\pi^* \leftarrow n$ transition, with much of the nonbonding electron density localized in the oxygen $2p_y$ orbital and with the π, π^* orbitals largely localized on the carbonyl in the *xz* plane (cf. Fig. 4).[19,41–43] However, a diverse range of views has been expressed concerning the detailed nature of the electric and magnetic moments accompanying the $\pi^* \leftarrow n$ transition, with regard to the carbonyl group as a chromophore in general and specifically with regard to the vapor phase (cf. Fig. 1) and solution (ethanol, hexane, and cyclohexane) spectra[22,23] of (+)-D-camphor. Most spectroscopic studies have followed a C_{2v} point group analysis of the carbonyl chromophore and have relied on analogies drawn with the homologous formaldehyde.[44]

The inhomogeneous dissymmetry observed for (+)-D-camphor has been a major focal point in rationalizing the observed oscillator and rotational strengths, insofar as the absorption and circular dichroism might arise from one or more identical or different components (*vide infra*) of the $\pi^* \leftarrow n$ transition mechanism. In contrast to Kuhn and Gore's[23] explanation of the inhomogeneous dissymmetry in terms of two absorption components, Moffitt and Moscowitz[11] explained it in terms of the circular dichroism being based on a totally symmetric vibronic progression with a 000 ← 000 origin and the absorption band being based upon a progression with asymmetric origin (100 ← 000).[45]

Gillard and Mitchell[22,46] in effect asserted the existence of some additional but undefined electric-dipole forbidden, magnetic-dipole allowed transition mechanism which would allow vibronic ϵ and $\Delta\epsilon$ bands to have

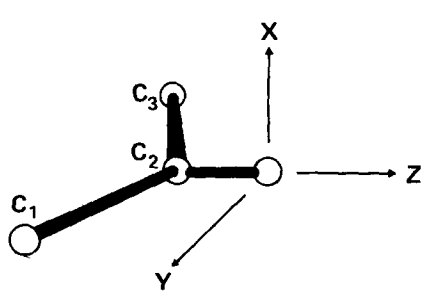

FIG. 4. Local oxygen centered coordinate system for defining carbonyl transition moment polarizations and the C_s and C_{2v} symmetry elements of Fig. 5. The C_1 $(C_2O)C_3$ array is here illustrated to be planar and thereby defines the *yz* plane.

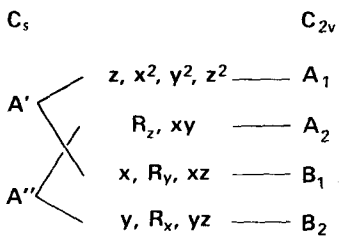

FIG. 5. Correlation table for the irreducible representations of the C_s and C_{2v} point groups as defined in the cartesian frame of Fig. 4.

identical band centers but inhomogeneous dissymmetry when evaluated bandwise over a vibronic progression.

In the past, only vibronic induction has been considered as a transition mechanism leading to the observed oscillator strengths. Most accounts cite Herzberg–Teller[47,48] vibronic admixture of the $\pi^* \leftarrow \pi$ and $\pi^* \leftarrow n$ transitions, and the vibronic electric moment resulting from such admixture is placed parallel with the carbonyl bond. Our own conclusion (*vide infra*) is that vibronically induced absorption intensity in (+)-D-camphor is not the only significant contribution to the observed oscillator strength. Rather, an important component of the $\pi^* \leftarrow n$ mechanism is electric-dipole allowed. In the sequel we refer to transition components which are distinguished on the basis of their associated progressions having either zero point ($0 \leftarrow 0$) or vibronically induced origins, where the induced components may arise because of symmetric or antisymmetric vibrations. Furthermore, since in the present treatment we presume that vibrational quantum numbers retain their validity and that absorption and circular dichroism are one-electron (single photon) processes, we consider the magnitudes and polarizations of electric and magnetic transition moments associated with each transition component. The electric and magnetic-dipole transition moments of each transition component are utilized as explicitly shown in Eqs. (2.1) and (2.2). The electric-dipole and quadrupole transition moments are used in the evaluation of the $V_{n_i m_j}$ coupling energies.

A. $00\nu_s \leftarrow 000$ component

First we recall a rule due to Herzberg,[48] that in all electric-dipole forbidden electronic transitions made possible by vibronic interaction, the $0 \leftarrow 0$ band is absent. However, the $000 \leftarrow 000$ band appears in the data of Fig. 1 as a shoulder in ϵ and as a corresponding peak in $\Delta\epsilon$, and there are similar occurrences in the spectra of (+)-D-camphor and isoandrosterone in cyclohexane[22] and of 3β-hydroxy-5α-androstan-16-one in methanol.[19] These spectra have comparable oscillator and rotational strengths ($\epsilon_{max} \sim 20$–35, $\Delta\epsilon_{max} \sim 1.5$–$5$), and the spacings in the ensuing vibronic progressions are all in the range of 1100-1200 cm^{-1}. The assignment[22] of the $00\nu_s \leftarrow 000$ progression in the symmetric excited state stretching vibration ($\nu_s' \sim 1100$ cm^{-1}) is based upon Brand's[44] analogous assignment in the spectrum of formaldehyde ($\nu_s' = 1182$ cm^{-1}). The ground state symmetric stretching frequencies (ν_s'') are 1740 and 1744 cm^{-1} for camphor[49] and formaldehyde, respectively.

Second, support for the electric-dipole allowedness of $\pi^* \leftarrow n$ transitions may be found in the work of Robin *et al.*[50] on *trans*azoalkanes. In their configuration interaction calculations it was found that vibronic mixing could account for only 14% of the theoretical oscillator strength. It is satisfying to note that the $\pi^* \leftarrow n$ transition, A_2 in C_{2v}, correlates (cf. Fig. 5) with the A'' representation in C_s, and that this pyramidal lowering of symmetry (cf. Sec. III) results in a slight electric-dipole allowedness as a zero-point effect. We may point to the ϵ and $\Delta\epsilon$ data[19] for 3β-hydroxy-5α-androstan-16-one ($\epsilon_{max} \sim 35$, $\Delta\epsilon_{max} \sim 5$) as a low absorption intensity example of a noncomplicated illustration of the Case I analysis[45] of Moffit and Moscowitz with *homogeneous* dissymmetry [$g(\nu) = 0.20 \pm 0.02$ between the $0 \leftarrow 0$ and $3 \leftarrow 0$ vibronic peaks]. In a very rough approximation, the homogeneous "calibration" given by this steroid data suggests that the $00\nu_s \leftarrow 000$ transition component may well account for about half of the experimental oscillator strength ($\sim 3.8 \times 10^{-4}$) in the (+)-D-camphor system.

The Herzberg rule cited above applies rigorously only in the absence of rotational–electronic interaction, and further analysis is required since it has been shown that the $0 \leftarrow 0$ band oscillator strength in formaldehyde derives from a magnetic-dipole transition.[51,52] From the steroid and camphor data,[19,22] we estimate the oscillator strength of the $000 \leftarrow 000$ member to be about 3×10^{-5}. Pople and Sidman[53] found in the case of formaldehyde that a maximal rotational–electronic interaction contribution of 10^{-6} could be made to the oscillator strength of the entire $\pi^* \leftarrow n$ absorption system. Since the least moment of inertia in camphor[49] is 6×10^{-38} g cm^2 and that for formaldehyde is 3×10^{-40} g cm^2, we expect that rotational–electronic interaction contributes no more than 5×10^{-9} to the camphor $000 \leftarrow 000$ oscillator strength and hence is negligible. The oscillator strength of the magnetic-dipole $0 \leftarrow 0$ member in formaldehyde[51] is less than 5×10^{-7}, and hence the $000 \leftarrow 000$ absorption band of camphor is predominantly not due to a magnetic-dipole transition. The rigorous application of the Herzberg rule is hence permitted, and the $00\nu_s \leftarrow 000$ transition component is therefore electric-dipole allowed (cf. Fig. 5) with y polarization in the frame of Fig. 4.

The magnetic-dipole transition moment referred to above is z polarized and symmetry allowed in both C_{2v} and C_s point groups. It is generally agreed that this moment is on the order of 1 μ_B for the carbonyl group in general, as deduced from simple AO and SCF–LCAO calculations[19] and from experiment.[51] An additional magnetic-dipole transition moment polarized in the x direction is symmetry allowed in C_s. From a two-center LCAO calculation of the second center (carbon C_2) contribution to a magnetic moment,[54] we would expect an x polarized moment on the order of 0.3 μ_B if the C_2 carbon AO contribution to the π^* orbital were a full $2p_z$ function. From our pyramidal distortion discussion of Sec. III and a maximal nonplanarity of 4.6°, we would expect that the fractional projection of the C_2 carbon $2p_z$ AO into the π^* orbital is less than 6%. We therefore estimate the x polarized magnetic-dipole moment to be less than 0.02 μ_B, which is sufficiently small in comparison to the z polarized component for us to neglect its contribution to the circular dichroism in our calculations.

The electric xy quadrupole transition moment has been estimated to be on the order of $0.6-8.1\times10^{-36}$ (cgs units),[10] and undergoes interactions of up to 1000 cm^{-1} with parts of the CC and CH densities of states (cf. Sec. V). The C_s symmetry allowed yz quadrupole moment is thus estimated to be less than 8×10^{-38} (cgs units), where an oxygen center expansion coefficient[55] for the $2p_z C_2$ carbon orbital of 0.13 and a 0.06 projection of the C_2 $2p_z$ onto π^* were invoked in formulating the inequality. The interaction contribution of the yz quadrupole was neglected in our calculations on the $00\nu_s \leftarrow 000$ component bands; all higher order multipolar transition moments were also neglected.

B. $00\nu_s \leftarrow 0\nu_{a'}0$ and $00\nu_s \leftarrow \nu_{a''}00$ components

In considering the qualitative effects of Herzberg–Teller vibronic intensity borrowing, we follow the form of the theory made explicit by Albrecht,[56] with the exception that in addition to the vibronically induced admixture of excited (virtual) carbonyl states into the π^* state (e.g., the $A''\sigma^* \leftarrow n$ transition), we consider also the admixture of initial (bound) states (e.g., the $A'\pi^* \leftarrow \pi$ transition). Since the $\pi^* \leftarrow n$ transition in zeroth order is A'', symmetric (a') vibrations will mix in A'' transitions, and the resulting induced transition moments will have identical polarizations to those discussed previously for the $00\nu_s \leftarrow 000$ component; the vibronic species are identical in the two types of components although the origins of the progressions differ by $\nu_{a'}$ vibrational quanta. Similarly, odd quanta of antisymmetric (a'') vibrations will mix in A' transitions and result in induced transition moments having polarizations characteristic of the admixed A' transition, which components are symmetry forbidden in the zeroth order $\pi^* \leftarrow n$ transition. It can be stated in general with certainty that in weakly absorbing systems it is not possible to distinguish, on the basis of symmetry arguments alone, which of the possible component transition mechanisms will dominate.[47] Vibronic mixing of the Herzberg–Teller type depends on the separation of zeroth-order electronic states being mixed, the transition moment magnitudes of the admixed transitions, and upon the detailed nature of the zeroth-order electronic functions over the amplitudes of nuclear (vibrational) displacement.[56] This is to say that rigorously the perturbational corrections should be included in the zeroth-order Hamiltonian.[57] However quite a few approximating quantitative treatments[53,58,59] have proven useful in qualifying the nature of vibronically induced electronic transition moments, and we will draw analogies to some of these treatments in our empirical analysis of camphor, especially in reference to the formaldehyde study by Pople and Sidman.[53]

1. *Perturbing vibrations*

We consider the normal vibrations of the $C_1(C_2O)C_3$ array in (+)-D-camphor in the context of an X_2CO molecule having C_s point group symmetry where the X atoms (C_1 and C_3) are considered to have adjustable effective masses. A theoretical normal mode analysis[60,61] indicates that for intermediate (6–15 amu's) effective masses the nominally in plane a'' bending (carbonyl wagging) mode will lie below a nominally in plane a' bending (C_1–C_3 scissor) mode in the range of 300–600 cm^{-1}. This result is in good qualitative agreement with vibrational spectra reported for aromatic, aliphatic, and cyclic ketones by Katon and Bentley[62] who suggested the out of plane a' bending mode in acetone lies below the above mentioned a'' mode.

These modes are sufficiently low in frequency so that even at room temperature the corresponding Boltzmann factors may be considered to be "favorable," and hence we focus our attention on singly thermally populated progressions ($\nu_{a'} = \nu_{a''} = 1$). These modes differ strikingly from those in formaldehyde, where the a'' mode occurs at 1280 cm^{-1}, and the a' modes occur at 1167 (out of plane bending) and 1503 cm^{-1}. These differences may reliably be attributed to effective mass differences.

The treatment of Pople and Sidman considered only zero-point perturbations in the normal coordinates. In the harmonic oscillator approximation, the vibronic interaction energy is proportional to the mean square displacement,[58] and hence proportional to[63] $v+\frac{1}{2}$, where v are the number of vibrational quanta excited. Hence hot states are expected to be three times as effective as zero-point vibrations in borrowing absorption intensity.

2. *$00\nu_s \leftarrow 010$ transition moments*

The polarizations for the electric and magnetic moments induced by the a' vibrations are identical to those of the $00\nu_s \leftarrow 000$ component. It is likely that the $(3s)\sigma^* \leftarrow n$ zeroth-order transition (~7 eV) will in this component provide most of the borrowed intensity. Pople and Sidman estimated that approximately 1% of the $\sigma^* \leftarrow n$ oscillator strength could be borrowed by out of plane vibrations in formaldehyde, which borrowing amounted to a vibronic oscillator strength of 3×10^{-4}. If we extrapolate upon the order of magnitude of this effect, the associated borrowing in the magnetic-dipole oscillator strength would be negligible in comparison to that which is allowed in the $00\nu_s \leftarrow 000$ component. Hence we may neglect borrowed rotational strength which arises from $\mu_e\mu_m$ coupling. The possibly $3s$ Rydberg nature[64] of the $\sigma^* \leftarrow n$ intervalence transition would further decrease the relative magnitudes of the borrowed magnetic-dipole and electric-quadrupole moments relative to the borrowed electric-dipole moment.

3. *$00\nu_s \leftarrow 100$ transition moments*

Intensity borrowing from the $\pi^* \leftarrow \pi$ transition (~8 eV) by "in plane" a'' vibrations is expected in C_s symmetry, and the resulting electric-dipole transition moment is z polarized. We will avoid guessing at the magnitude of the borrowed electric-dipole oscillator strength, but we stress the following point. No magnetic-dipole strength is borrowed.

C. Circular dichroic consequences of vibronic borrowing

We suggest that to first-order in the Herzberg–Teller theory, vibronic borrowing of electric-dipole oscillator strength is inseparable from the borrowing of all other electric and magnetic moments associated with the ad-

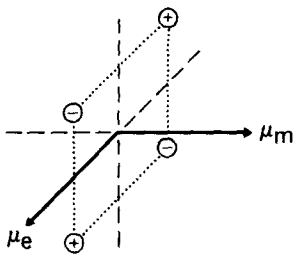

FIG. 6. Principal transition moments of the $00v_s \leftarrow 000$ $\pi^* \leftarrow n$ component in the frame of Fig. 4 where μ_m is oriented in the z direction, μ_e is oriented in the y direction, and the four monopoles lying in the xy plane define the corresponding xy electric quadrupole. The arrow orientations and the monopole signs illustrate the correct relative phases of the three different moments (cf. Ref. 66).

mixed transition. This view is rigorous within the confines of the applicability of group theoretical labels. Independent support can be taken from the work of Denning,[65] who referred to circular dichroism borrowing. Under the qualified assumptions we have made above, we expect that the $00v_s \leftarrow 0v_{a'}0$ and $00v_s \leftarrow v_{a''}00$ transition components will make a negligible $\mu_e\mu_m$-coupling contribution to $\Delta\epsilon$, as a consequence of negligible borrowed magnetic-dipole oscillator strengths, and hence the borrowed circular dichroism will be limited to that generated from the borrowed electric-dipole transition moment in a $\mu_e\mu_e$-coupled mechanism. It is obvious that the rotational-strength sum rule is preserved. We expect that the borrowed electric-dipole oscillator strength to be competitive with that accompanying the $00v_s \leftarrow 000$ component of the $\pi^* \leftarrow n$ transition mechanism, and further that the y-polarized electric-dipole, z-polarized magnetic-dipole, and xy electric-quadrupole transition moments of the $00v_s \leftarrow 000$ component will be chiefly responsible for the circular dichroism.

V. RANDOM-PHASE CALCULATIONS

The implementation of Eqs. (2.1) and (2.2) in calculating $\epsilon(\nu)$ and $\Delta\epsilon(\nu)$ is straightforward for any given parameterization. Certain of the parameters are fixed by experiment (e.g., vibronic band structure constants and most of the atomic coordinates) and theory (e.g., bond polarizabilities), and some of the parameters are rather arbitrary (e.g., charge separations used in making the monopole array approximation to the transition charge densities). Therefore the purpose of the present section is to illustrate the general validity of our model in accounting for the experimental $\Delta\epsilon$, to illustrate the insensitivity of the calculated results upon the arbitrary parameters, to investigate the relative importance of the $\mu_e\mu_e$ and $\mu_e\mu_m$ coupling mechanisms in determining the $\Delta\epsilon$, and to examine the factors which predominate in the coupling as influenced by conformation, transition moment magnitudes, etc. In the following we define a reference parameterization and then present results for excursions made in various parameter classes.

Our reference electric-dipole, electric-quadrupole, and magnetic-dipole transition moments for the $00v_s \leftarrow 000$ ($v_s = 0, 1, 2$, and 3) progression in the $\pi^* \leftarrow n$ transition are centered on the oxygen nucleus with the relative orientations and phases illustrated in Fig. 6. Monopoles are also distributed for the μ_e moment, and these dipole and quadrupole monopole arrays are then coupled with the monopole arrays of the backbone dipoles in computing the $V_{n_1m_2}$ interaction energies. The relative Franck–Condon factors for each of the vibronic bands, presumed to be reflected in the resultant experimental circular dichroism, were used in scaling all of the vibronic transition moments. The zero-point vibronic oscillator strength ($000 \leftarrow 000$) was set at 3×10^{-5} so that the resulting absorption envelope calculated would have $\epsilon_{max} \sim 20$. In this computational approximation, almost all of the experimentally observed oscillator strength was attributed to the $00v_s \leftarrow 000$ progression, and this approximation serves to set an upper bound for certain of the effects discussed in the sequel. The associated $001 \leftarrow 000$ magnetic-dipole moment was fixed at 1 μ_B and the corresponding xy quadrupole moment was fixed (mid-range) at 4×10^{-26} (cgs units).

In conjunction with the specified electric-dipole transition moment vectors, the magnitudes of the monopoles are determined by a specification of the charge separation and likewise for the quadrupole arrays of monopoles. The polarizability of each CC and CH bond is represented by a set of three orthogonal electric-dipole transition moments centered on the midpoints of the bonds, with the parallel component oriented along the bond and with the perpendicular axes oriented arbitrarily in a perpendicular plane. The magnitudes of the associated parallel and perpendicular moments were scaled to give the zero frequency anisotropy and polarizability subsequent to the specification of the corresponding band center frequency and half-width common to all of the polarizability approximating transition-dipoles. The reference atomic coordinates are those of Table I with the carbonyl in plane and the methyl groups in staggered positions. The qualitative effects of the pyramidal distortions in the $C_1(C_2O)C_3$ array are explicitly investigated. The reference parameterization is summarized in Table II.

The ϵ and $\Delta\epsilon$ spectra calculated with the reference parameterization are illustrated in Fig. 7. In this calculation we have assumed that all of the oscillator strength results from the allowed $00v_s \leftarrow 000$ transition moments. This assumption is contrary to our analysis of the previous section, but for the purposes of discussion it serves to establish an upper bound for the effects of the $\langle A''(\pi^*, n)00v_s|\hat{\mu}_e|A'(n^2)000\rangle$ transition moments on the resulting $\Delta\epsilon$, as is explained below. Moreover, we have assumed a planar reference geometry after stressing the existence of a slight zero-point pyramidal distortion. Since the strongest evidence for this distortion is spectroscopic and the x-ray data do not indicate in which direction the distortion occurs, we have chosen the in-plane structure as a reference geometry while retaining a C_s basis. Hence the exact nature and extent of the pyramidal distortion is only expected to affect slightly the corresponding scalar- and cross-products among the transition moments and the Coulombic interactions among the transition charge densities.

The calculated absorption coefficients in Fig. 7 are the sums of both the zeroth and first-order terms of

TABLE II. Reference parameterization for the random-phase calculations.

Vibronic structure
$0 \leftarrow 0$ oscillator strength: 3×10^{-5}
Relative Franck-Condon factors: 0.74 ($0 \leftarrow 0$), 1.0 ($1 \leftarrow 0$), 0.90 ($2 \leftarrow 0$), 0.54 ($3 \leftarrow 0$)
Magnetic-dipole transition moment ($1 \leftarrow 0$) band): 1 μ_B
xy electric-quadrupole transition moment ($1 \leftarrow 0$ band): 4×10^{-26} (cgs units)
Transition moment orientations: see Fig. 6
Band centers (cm^{-1}): 31 950 ($0 \leftarrow 0$), 33 050 ($1 \leftarrow 0$), 34 050 ($2 \leftarrow 0$), 35 100 ($3 \leftarrow 0$)
Half-widths: 1000 cm^{-1}
Polarizability approximation
CH bonds: 10.99×10^{-25} cm^3 ($\parallel$), 6.40×10^{-25} cm^3 ($\perp$)
CC bonds: 7.56×10^{-25} cm^3 ($\parallel$), 3.95×10^{-25} cm^3 ($\perp$)
Band center: 10^5 cm^{-1}
Half-widths: 200 cm^{-1}
Transition moment charge separations
CO, CH, amd CC μ_e: 0.1 Å (a)
CO xy electric-quadrupole along diagonals (cf. Fig. 6): $\sqrt{2}/5$ Å ($2\sqrt{2}a$)
Conformational geometry
Atomic coordinates: see Fig. 3 and Table I
Carbonyl orientation: in $C_1(C_2O)C_3$ plane
Methyl groups: staggered

Eq. (2.1). In this case the first-order terms were uniformly on the order of 40% of the zeroth-order contributions, the effects of the coupling through the polarizability approximation being hyperchromic. The circular dichroism illustrated in Fig. 7 is the sum of contributions from both the $\mu_e\mu_e$- and $\mu_e\mu_m$-coupling mechanisms. In this case the $\mu_e\mu_e$-coupling contribution goes counter to the $\mu_e\mu_m$-coupling $\Delta\epsilon$, where $\mu_e\mu_e$-coupling $\Delta\epsilon$ is on the order of -7% of that due to $\mu_e\mu_m$-coupling. Since we may have overestimated the oscillator strength of the $00v_s \leftarrow 000$ system, it is seen that the $\mu_e\mu_e$-coupling mechanism plays an insignificant role in the resulting circular dichroism. In Fig. 8 we have illustrated the decomposition of the $\Delta\epsilon$ arising from $\mu_e\mu_m$-coupling, into the constituent components of the transition charge density Coulombic interaction energy. If the $\pi^* \leftarrow n$ transition were in fact electric-dipole forbidden, the leading term in the interacting transition charge density would be quadrupole. In the present case the leading term is dipolar, and so we are comparing in Fig. 8 the relative contributions to the $\mu_e\mu_m$-coupling $\Delta\epsilon$ of the dipole and quadrupole components of the coupling energy. The energetics are seen to be dominated by the quadrupolar contribution, and the dipole contribution induces in $\Delta\epsilon$ a term of opposite sign. Since each of the components illustrated is linearly proportional to either the (electric) dipole or quadrupole transition moments and the corresponding magnetic-dipole moment appears identically in expressions for each component, the question of the dominant component of the associated transition charge density field must also be investigated within the context of $\mu_e\mu_e$ or $\mu_e\mu_m$ mechanisms. While it is the quadrupolar component which clearly dominates in this case, there is no indication that extrapolation of this effect to other systems is justified in the absence of accompanying absorption data. This case illustrates, however, that it is important to keep the correct relative phases of transition moments associated with a given transition (i.e., to use the same eigenfunctions in evaluating a set of expectation values).[66] Otherwise, in the present case the electric-dipole and electric-quadrupole interaction contributions would be reinforcing rather than opposing. Significant error might incur in other cases where the magnitudes of the competing contributions were not so dissimilar. The random-phase approximation invoked in the TDH theory has to do solely with the relative phases of any two transitions on different groups.

At this point it is appropriate to show that in our calculations the (arbitrary) "parameters that shouldn't matter don't." Specifically, we refer to the band structural parameters in the polarizability approximation

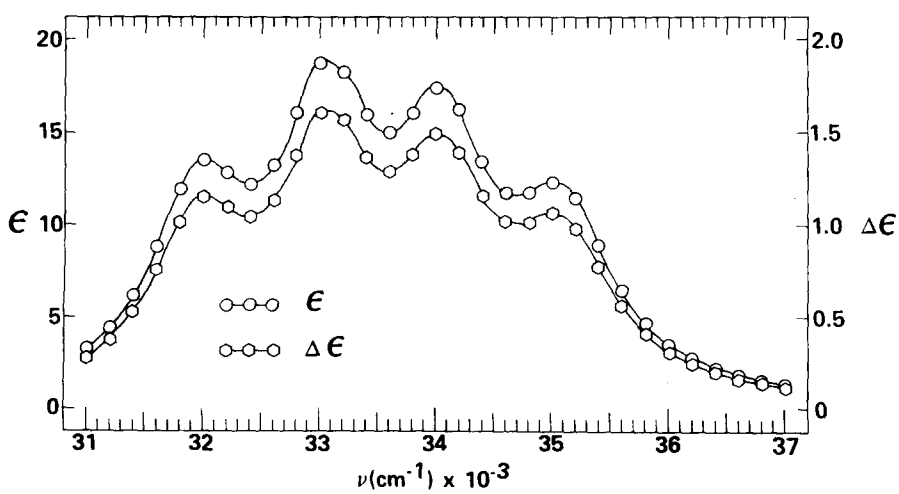

FIG. 7. Calculated total absorption and circular dichroism of the $00v_s \leftarrow 000$ component in the reference parameterization (cf. Table II). The circular dichroism illustrated is 98% due to $\mu_e\mu_m$ coupling.

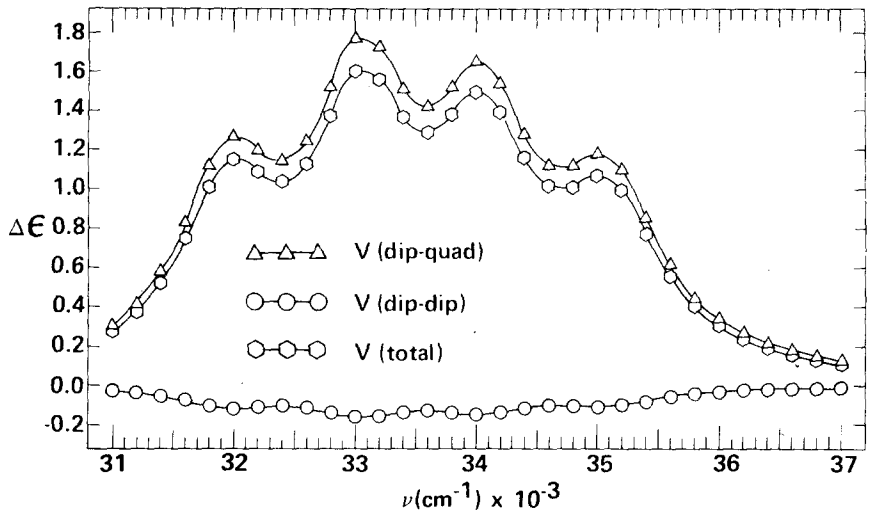

FIG. 8. Decomposition of the calculated (reference parameterization, cf. Table II) circular dichroism of Fig. 7 into components which arise from the separable coupling energies of the $00\nu_s \leftarrow 000$ transitions with the backbone CC and CH polarizabilities through the carbonyl electric-dipole (dip–dip) and electric–quadrupole (dip–quad) transition moments.

and to the charge separations used in classically approximating the electrostatic transition charge densities. The absorption threshold for aliphatic CC and CH bonds lies above 68 000 cm^{-1} and hence makes only a very small contribution to the imaginary part of the molecular susceptibility in the 3000 Å range of the $\pi^* \leftarrow n$ transition. Of much greater importance is the dispersion of the associated polarizability in the region of our calculations. Snyder and Johnson[32] have pointed out that it is not generally possible to exactly reproduce the proper polarizability in a nonabsorbing region by scaling a supertransition to give the correct zero-frequency polarizability, although the approximating practice is generally accepted. At any rate, we note the following effects of varying the supertransition band centers and half-widths, keeping other parameters fixed as in Table II. Increasing the band center to 200 000 cm^{-1} and decreasing the band center to 75 000 cm^{-1} resulted in a 9% decrease and a 9% increase, respectively, in ϵ_{max} (33 000 cm^{-1}), and a 13% decrease and a 13% increase, respectively, in $\Delta\epsilon$ (37 000 cm^{-1}) at the high energy limit of our calculations. Analogous changes in the low energy wing of the band were less than 8% in $\Delta\epsilon$ (30 000 cm^{-1}). Thus only a very slightly inhomogeneous variation, on the order of 10%, is induced in the calculated $\Delta\epsilon$ with extremely wide variations in our choice of ν_{ST}. Increasing the associated half-width to 40 000 cm^{-1} and decreasing the half-width to 10 cm^{-1} changed $\Delta\epsilon_{max}$ by less than 1%. Thus it is likely that the most severe error induced by the polarizability approximation is not in our choice of band structure constants and our zero-frequency scaling but in our choice of the zero-frequency polarizabilities themselves, which vary by as much as 25% among different experimental and theoretical values cited by Amos and Crispen.[36] Our assumption of group separability is likely to be more severe here in the "small molecule" case than in the case of polymers for which the random-phase approach has already been successfully applied. An accompanying approximation is that there is no overlap between the transition charge densities on the different groups,[67] and hence that the transition charge densities may be modeled classically by an array of monopoles. In this approximation we need to check that no artifacts are introduced into the evaluation of the dipole–dipole and dipole–quadrupole transition charge density interactions by having the corresponding monopoles placed too far apart. We found that increasing the charge separations to $a = 1.00$ Å resulted in less than a 3% decrease in the calculated $\Delta\epsilon_{max}$.

The most severe effects that we observed for parameter variations not relating to transition moment magnitudes were geometrical. When we lowered the carbonyl bond axis 4.6° below ($-x$ direction in Fig. 4) the $C_1(C_2O)C_3$ plane, a 17% decrease in $\Delta\epsilon_{max}$ ensued. Likewise, raising the oxygen an identical amount above the plane resulted in a 17% increase in $\Delta\epsilon_{max}$. We are unable to tell which of these pyramidal distortions is most favored. Changing the methyl group orientations from being locally staggered to eclipsed resulted in a decrease in $\Delta\epsilon_{max}$ to 0.6. However, a very conservative estimate of 1 kcal/mol for the eclipsed rotational barrier in these methyl groups makes the Boltzmann averaged contributions of the eclipsed conformations to the calculated spectra almost negligible.

Since the overall rotational strengths calculated are dominated by dipole–quadrupole coupling in the $\mu_e\mu_m$-coupling mechanism, it is instructive to investigate the relative contributions induced by the separate CC and CH bonds in terms of the associated xy quadrant projection. The quadrant numbering scheme is illustrated in Fig. 9. In Table III we list the relative contributions of each CC and CH bond to the total calculated rotational strength, which quantities are expressed fractionally as (bond contribution)/(sum of all contributions). Inspection of Table III indicates that a quadrant rule is followed faithfully, with three exceptions involving bonds which cross quadrant planes (i.e., C_4H_{4-1}, C_8H_{8-3}, $C_{10}H_{10-3}$). It is interesting to note further than the CC bonds as a whole account for 17% of the calculated rotational strength, and in Fig. 9 we illustrate the quadrant contributions to the rotational strength and the decomposition of these contributions into components induced by CC and CH bonds, respectively.

It appears that in the present method of calculation,

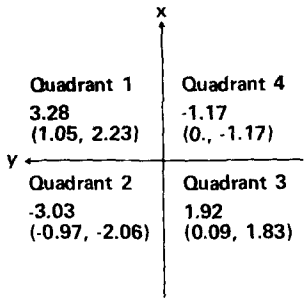

FIG. 9. Quadrants associated with the xy electric-quadrupole of Fig. 6 in the frame of Fig. 4. The quadrant positions of the atoms and bond centers are given in Tables I and III, respectively. Indicated in each quadrant are the relative contributions to the V (dip–quad) coupled rotational strengths (cf. Fig. 8 and Table III) for all of the backbone bonds in each quadrant. The values in parentheses are the relative contributions of the CC and CH bonds, respectively, in each quadrant.

the most critical parameters are the transition moments, as we had hoped. Implicit errors in the zero-frequency polarizabilities will not affect the signs of the calculated rotational strengths, since we have shown that net CC and CH bond contributions are of the same sign. Moreover, the xy quadrupole moment used herein is midrange in magnitude with respect to accepted theoretical and experimental values. We have shown that this quadrupole transition moment dominates the present optical rotatory mechanism in $\mu_e\mu_m$-coupling, and the net calculated $\Delta\epsilon$ is roughly linearly proportional to the quadrupole moment magnitude selected and hence also the magnetic moment.

The calculated $\Delta\epsilon$ arising from the $00v_s \leftarrow 0v_{a'}0$ and $00v_s \leftarrow v_{a''}00$ components in the $\mu_e\mu_e$-coupling limit (assuming the reference oscillator strengths) was found to be less than 2% of the total calculated for the $00v_s \leftarrow 000$

TABLE III. Bond polarizability contributions to the calculated rotational strength of the $0 \leftarrow 0$ component of the $\pi^* \leftarrow n$ band due to dipole (backbone)–quadrupole (carbonyl) coupling.

Bond	Transition center quadrant	Rotational strength Bond total rotational strength	
C_1–C_2	0	0.	
C_2–C_3	0	0.	
C_3–C_4	3	0.05	
C_4–C_5	3	0.04	
C_5–C_6	2	−0.35	
C_6–C_1	2	−0.62	
C_1–C_7	1	0.23	
C_4–C_7	1	0.00	
C_7–C_8	1	0.13	
C_7–C_9	1	0.08	
C_1–C_{10}	1	0.61	
			0.17[a]
C_3–H_3–1	4	−1.18	
C_3–H_3–2	3	1.74	
C_4–H_4–1	4	0.01	
C_5–H_5–1	2	−0.03	
C_5–H_5–2	3	0.08	
C_6–H_6–1	2	−0.65	
C_6–H_6–2	2	−1.38	
C_8–H_8–1	1	0.09	
C_8–H_8–2	1	0.28	
C_8–H_8–3	1	−0.20	
C_9–H_9–1	1	0.04	
C_9–H_9–2	1	0.07	
C_9–H_9–3	1	0.02	
C_{10}–H_{10}–1	1	1.66	
C_{10}–H_{10}–2	1	0.58	
C_{10}–H_{10}–3	1	−0.31	
			0.83[b]

[a]Fractional contribution of CC bonds.
[b]Fractional contribution of CH bonds.

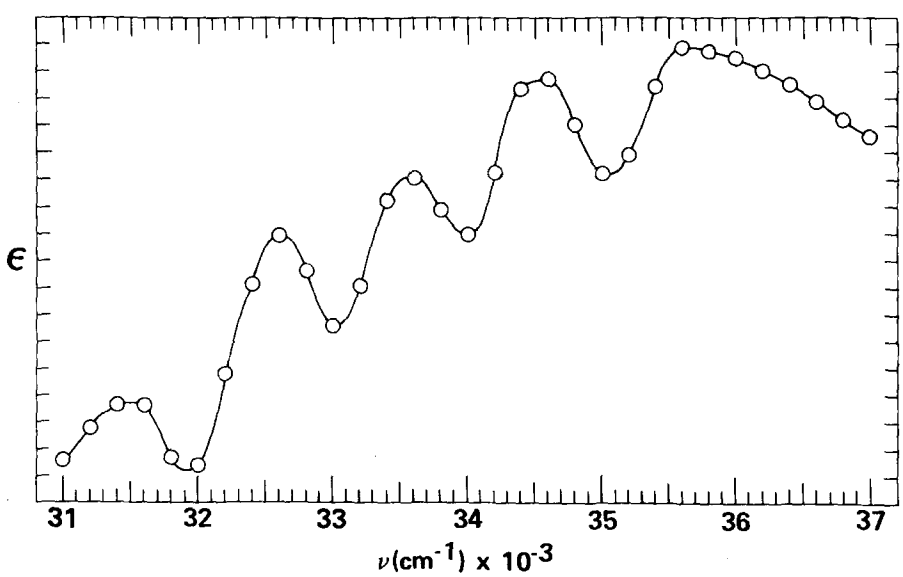

FIG. 10. Resulting band profile from the subtraction of the calculated absorption due to the $00v_s \leftarrow 000$ component of Fig. 7 from the experimental absorption of Fig. 1. A slight background continuum connecting to the backbone density of states has not been subtracted. The hot band at 31 500 cm^{-1} is displaced about 400–500 cm^{-1} to the red of the $0 \leftarrow 0$ origin as would be expected for an average of the $\nu''_{a'}$ and $\nu''_{a''}$ frequencies discussed in Sec. IV.B. The approximately 600 cm^{-1} displacement to the blue of the $0 \leftarrow 0$ origin indicates the average of $\nu'_{a'}$ and $\nu'_{a''}$. The 1000 cm^{-1} separation between the hot band and first main band is inconsistent with any ground state fundamental frequency other than the second a'' vibration which is likely greater than 1000 cm^{-1} (cf. Ref. 60) and which would violate the selection rule pertaining to allowed transitions between antisymmetric modes ($\sum \Delta v_{a''} = 0, \pm 2, \ldots$).

component. This result is consistent with our qualitative summary of Sec. IV. C, and the associated error therefore is majorized by bounds placed on borrowed magnetic-dipole oscillator strength.

In returning to the question of dissymmetry, we compare in Fig. 2 the experimental values with those obtained by dividing our calculated (reference parameters) $\Delta\epsilon$ by the experimental absorption. Since we have presumed the existence of vibronically induced intensity borrowing in addition to the calculated absorption, the agreement illustrated in Fig. 2 confirms the fidelity of our choice of vibronic band structural parameters. More interesting is the band profile obtained by subtracting our calculated absorption curve in Fig. 7 from the experimental absorption (scaled to have $\epsilon_{max} \sim 30$). This difference "spectrum" is illustrated in Fig. 10 and exhibits several of the features predicted for underlying $00v_s \leftarrow 0v_a, 0$ and $00v_s \leftarrow v_a, 00$ progressions. These vibrations are on the order of 400–500 cm^{-1}, and the low frequency intensity at about 31 400 cm^{-1} and the greater intensity at about 32 500 cm^{-1} are, respectively, consistent with hot bands and displaced origins. Above 32 500 cm^{-1} there is a progression with spacings on the order of 1100–1200 cm^{-1}. Our empirical analysis of the dissymmetry therefore appears to be at least qualitatively consistent.

VI. SUMMARY

The random-phase time-dependent Hartree theory has been successfully applied in the independent systems approximation to the calculation of the 3000 Å circular dichroism band of (+)-D-camphor. The dominant mechanism has been shown to be due to $\mu_e\mu_m$-coupling, and this coupling itself is dominated by the interaction of the $\langle A''(\pi^*, n)00v_s | xy | A'(n^2)000\rangle$ electric-quadrupole transition charge density with the CC and CH backbone densities of states. This study lends some additional validity to analogous studies of Höhn and Weigang, where the competitive effects of associated electric-dipole coupling mechanisms were not investigated. Use of the most general vibronic selection rules indicates that the experimental absorption envelope is comprised of intensity competitive electric-dipole allowed and vibronically allowed contributions. The accompanying circular dichroism band, however, is based rather extensively on the electric-dipole allowed transition components. We find therefore that the original explanation of Kuhn and Gore for the inhomogeneous dissymmetry, namely, the existence of an adjacent band in absorption, is most probably correct and is consistent with our empirical analysis of overlapping vibronically induced progressions. In conclusion it is reiterated that the use of Herzberg–Teller absorption intensity borrowing mechanisms must be made with simultaneous considerations of associated circular dichroism intensity quenching effects.

[1]J. A. Schellman, Acc. Chem. Res. 1, 144 (1968).
[2]W. J. Kauzmann, J. E. Walter, and H. Eyring, Chem. Rev. 26, 339 (1940).
[3]W. Moffitt, R. B. Woodward, A. Moscowitz, W. Klyne, and C. Djerassi, J. Am. Chem. Soc. 83, 4013 (1961).
[4]A. Moscowitz, Adv. Chem. Phys. 4, 67 (1962).
[5]W. Kuhn, Trans. Faraday Soc. 26, 293 (1930).
[6]W. Kuhn, Ann. Rev. Phys. Chem. 9, 417 (1958).
[7]J. G. Kirkwood, J. Chem. Phys. 5, 479 (1937).
[8]J. A. Schellman, J. Chem. Phys. 44, 55 (1966).
[9]E. U. Condon, W. Altar, and H. Eyring, J. Chem. Phys. 5, 753 (1937).
[10]E. G. Höhn and O. E. Weigang, Jr., J. Chem. Phys. 48, 1127 (1968).
[11]W. Moffitt and A. Moscowitz, J. Chem. Phys. 30, 648 (1959).
[12]W. Moffitt, J. Chem. Phys. 25, 467 (1956).
[13]W. Moffitt, D. D. Fitts, and J. G. Kirkwood, Proc. Natl. Acad. Sci., U.S.A. 43, 723 (1957).
[14]W. Moffitt, D. D. Fitts, and J. G. Kirkwood, Proc. Natl. Acad. Sci., U.S.A. 43, 1046 (1957).
[15]S. H. Lin, J. Chem. Phys. 55, 3546 (1971).
[16]"Optical Rotatory Dispersion and Circular Dichroism in Organic Chemistry," edited by G. Snatzke (Heydon, London, 1967).
[17]D. E. Bays, G. W. Cannon, and R. C. Cookson, J. Chem. Soc. B. 1966, 885.
[18]L. Bartlett, D. N. Kirk, W. Klyne, S. R. Wallis, H. Erdtman, and S. Thoren, J. Chem. Soc. C. 1970, 2678.
[19]S. F. Mason, Mol. Phys. 5, 343 (1962).
[20]A. Moscowitz, in Ref. 16, pp. 41–70.
[21]L. C. Snyder and A. Moscowitz, unpublished results presented in Ref. 20.
[22]R. D. Gillard and P. R. Mitchell, Trans. Faraday Soc. 65, 2611 (1969).
[23]W. Kuhn and H. K. Gore, Z. Phys. Chem. (Leipzig) B 12, 389 (1931).
[24]A. D. McLachlan, R. D. Gregory, and M. A. Ball, Mol. Phys. 7, 119 (1963).
[25]A. D. McLachlan and M. A. Ball, Mol. Phys. 8, 581 (1964).
[26]R. A. Harris, J. Chem. Phys. 43, 959 (1965).
[27]A. S. Schneider and R. A. Harris, J. Chem. Phys. 50, 5204 (1969).
[28]W. Rhodes, J. Chem. Phys. 53, 3650 (1970).
[29]A. R. Ziv and W. Rhodes, J. Chem. Phys. 57, 5354 (1972).
[30]E. S. Pysh and J. L. Richards, J. Chem. Phys. 57, 3680 (1972).
[31]E. S. Pysh, Biopolymers 13, 1563 (1974).
[32]P. A. Snyder and W. C. Johnson, Jr., J. Chem. Phys. 59, 2618 (1973).
[33]J. Applequist, J. Chem. Phys. 58, 4251 (1973).
[34]H. R. Dickenson, thesis, Oregon State University (1972).
[35]S. Rothenberg, J. Chem. Phys. 51, 3389 (1969).
[36]A. T. Amos and R. J. Crispen, J. Chem. Phys. 63, 1890 (1975).
[37]I. Tinoco, Adv. Chem. Phys. 4, 113 (1962).
[38]M. G. Northolt and J. H. Palm, Rec. Trav. Chim. 85, 143 (1966).
[39]F. H. Allen and D. Rogers, J. Chem. Soc. B. 1971, 632.
[40]J. A. Wunderlich, Acta Cryst. 23, 846 (1967).
[41]E. E. Barnes and W. T. Simpson, J. Chem. Phys. 39, 670 (1963).
[42]J. M. Foster and S. F. Boys, Rev. Mod. Phys. 32, 303 (1960).
[43]P. L. Goodfriend, F. W. Birss, and A. B. F. Duncan, Rev. Mod. Phys., 32, 307 (1960).
[44]J. C. D. Brand, J. Chem. Soc. 1958, 858.
[45]It thus represented their Case II treatment of vibronic structure in circular dichroism and absorption band shapes. Their Case I treatment of electric- and magnetic-dipole allowed transitions leads to a dissymmetry constant over the vibronic envelope except in the wings of absorption where $\Delta\epsilon$ decreases more rapidly than ϵ (cf. Refs. 11 and 15).
[46]In Ref. 22, the Case I conclusions of Moffitt and Moscowitz were apparently mistakenly identified with their Case II hypotheses, leading the authors to invoke an additional and unspecified case.

[47]G. Herzberg and E. Teller, Z. Phys. Chem. (Leipzig), B 21, 410 (1933).
[48]G. Herzberg, "Molecular Spectra and Molecular Structure. III. Electronic Spectra and Electronic Structure of Polyatomic Molecules," (Van Nostrand, Princeton, 1966).
[49]M. Jauquet and P. Laszlo, Chem. Phys. Lett. 15, 600 (1972).
[50]M. B. Robin, R. R. Hart, and N. A. Kuebler, J. Am. Chem. Soc. 89, 1564 (1967).
[51]J. H. Callomon and K. K. Innes, J. Mol. Spectrosc., 10, 166 (1963).
[52]J. R. Lombardi, D. E. Freeman, and W. Klemperer, J. Chem. Phys. 46, 2746 (1967).
[53]J. A. Pople and J. W. Sidman, J. Chem. Phys. 27, 1270 (1957).
[54]W. H. Flygare and V. W. Weiss, J. Chem. Phys. 45, 2785 (1966).
[55]P.-O Löwdin, Adv. Phys. 5, 1 (1956).
[56]A. C. Albrecht, J. Chem. Phys. 33, 156 (1960).
[57]R. Englman, "The Jahn-Teller Effect in Molecules and Crystals," (Wiley, London, 1972), p. 1.
[58]J. N. Murrell and J. A. Pople, Proc. Phys. Soc. A 69, 245 (1956).
[59]A. C. Albrecht, J. Chem. Phys. 33, 169 (1960), and references cited therein.
[60]G. Herzberg, "Molecular Spectra and Molecular Structure. II. Infrared and Raman Spectra of Polyatomic Molecules," (Van Nostrand, Princeton, 1960), pp. 65, 179–180, 199–201.
[61]O. Burkard, Proc. Ind. Acad. 8, 365 (1938).
[62]J. E. Katon and F. F. Bentley, Spectrochim. Acta 19, 639 (1963).
[63]H. Eyring, J. Walter, and G. E. Kimball, "Quantum Chemistry," (Wiley, New York, 1944), p. 79.
[64]M. B. Robin, "Higher Excited States of Polyatomic Molecules," (Academic, New York, 1975), Vol. II, Chap. IV.
[65]R. G. Denning, Chem. Commun. 120 (1967).
[66]C. W. Ufford and G. H. Shortley, Phys. Rev. 42, 167 (1932).
[67]H. C. Longuet-Higgins, Proc. R. Soc., A 235, 537 (1956).